Title: Internalization and vacuolar targeting of the brassinosteroid hormone receptor BRI1 are regulated by ubiquitination.
Authors: Martins S, Dohmann EM, Cayrel A, Johnson A, Fischer W, Pojer F, Satiat-Jeunemaître B, Jaillais Y, Chory J, Geldner N, Vert G
Journal: Nature communications
Year: 2015 Jan 21
Volume: 6
Pages: 6151
DOI: 10.1038/ncomms7151

HHS Public Access

Author manuscript

Nat Commun. Author manuscript; available in PMC 2016 January 14.

Published in final edited form as:

Nat Commun. ; 6: 6151. doi:10.1038/ncomms7151.

Dual role for ubiquitin in plant steroid hormone receptor endocytosis

Sara Martins[1], **Esther M. N. Dohmann**[2], **Jim Dompierre**[1], **Wolfgang Fischer**[3], **Florence Pojer**[4], **Yvon Jaillais**[5], **Béatrice Satiat-Jeunemaître**[1], **Joanne Chory**[3,6], **Niko Geldner**[2], and **Grégory Vert**[1,*]

[1]Institut des Sciences du Végétal, Saclay Plant Sciences, Centre National de la Recherche Scientifique Unité Propre de Recherche 2355, Avenue de la Terrasse, 91190 Gif-sur-Yvette, France. [2]Department of Plant Molecular Biology, University of Lausanne, UNIL-Sorge, 1015 Lausanne, Switzerland. [3]The Salk Institute for Biological Studies, 10010 North Torrey Pines Road, La Jolla CA 92037, USA. [4]Protein Crystallography Core Facility, Ecole Polytechnique Fédérale de Lausanne, SV 3827 Station 19, 1015 Lausanne, Switzerland. [5]Laboratoire de Reproduction et Développement des Plantes, INRA, CNRS, ENS Lyon, Université de Lyon, 46 allée d'Italie, 69364 Lyon Cedex 07, France. [6]Howard Hughes Medical Institute, The Salk Institute for Biological Studies, 10010 North Torrey Pines Road, La Jolla, CA 92037, USA.

Abstract

Brassinosteroids (BRs) are plant steroid hormones that control many aspects of plant growth and development. BRs are perceived at the cell-surface by the plasma membrane-localized receptor complex composed of the receptor kinase BRI1 and its co-receptor BAK1. Here we show that BRI1 is post-translationally modified by K63 polyubiquitin chains *in vivo*. Artificially ubiquitinated BRI1 is recognized at the *trans*-Golgi Network/Early Endosomes (TGN/EE) and rapidly routed for vacuolar degradation. Mass spectrometry analyses identified residue K866 as an *in vivo* ubiquitination target in BRI1 involved in the negative regulation of BRI1. Model prediction revealed several redundant ubiquitination sites required for the endosomal sorting and vacuolar targeting of BRI1. Using total internal reflection fluorescence microscopy (TIRF), we also uncovered a role for BRI1 ubiquitination in promoting internalization from the cell-surface. Finally, we demonstrate that the control of BRI1 protein dynamics by ubiquitination is a fundamental control mechanism for BR responses in plants. Altogether, our results identify K63-linked polyubiquitin chain formation as a dual targeting signal for BRI1 internalization and sorting along the endocytic pathway, and highlight its role in hormonally controlled plant development.

[*]To whom correspondence should be addressed. Gregory.Vert@isv.cnrs-gif.fr.

Author contributions

S.M., E.M.N.D., N.G. and G.V. designed the study; S.M., E.M.N.D, J.D., and W.F. performed experiments; F.P, J.D. and B.S.J gave technical support for model prediction and TIRF microscopy; Y.J. provided reagents; J.C. gave conceptual advice; G.V, Y.J, and N.G. wrote the manuscript.

Introduction

Brassinosteroids (BRs) are polyhydroxylated plant steroid hormones that regulate plant growth and development [1]. Studies of mutants with defects in BR biosynthesis or signaling demonstrated that BRs play essential roles in nearly all phases of plant development, as these mutants show multiple developmental defects, such as reduced seed germination, extreme dwarfism, photomorphogenesis in the dark, altered distribution of stomata, delayed flowering and male sterility [1, 2]. BRs are perceived at the cell surface by the membrane-bound receptor complex composed of the BRASSINOSTEROID INSENSITIVE1 (BRI1) receptor kinase and BRI1-ASSOCIATED RECEPTOR KINASE1 (BAK1) [3, 4, 5]. Ligand-dependent auto- and trans- phosphorylation of BRI1 and BAK1 participate in receptor complex activation and modulate a cellular cascade of kinases and phosphatases [6, 7], which ultimately culminates in the dephosphorylation and activation of two transcription factors, BRASSINAZOLE-RESISTANT1 (BZR1) and BRI1-EMS SUPPRESSOR1 (BES1) [8, 9]. BES1 and BZR1 bind to target promoters in the presence of different interacting partners to regulate BR genomic responses [10, 11, 12].

Adjustments in subcellular distribution of cell surface receptors are critical to modulate their signaling activity. Over the past decade, BRI1 has served as model for a better understanding of the interplay between receptor trafficking, signal transduction and deactivation. BRI1 constitutively cycles between the plasma membrane and the *trans*-Golgi network/early endosome (TGN/EE), and it is targeted to the vacuole for degradation *via* the late endosomes/multivesicular bodies (MVBs), independently of its ligand [13, 14]. The drug-mediated trapping of BRI1 in endosomes was shown to enhance BR responses, leading to a model whereby BRI1 signals preferentially from endosomal compartments [13]. This concept was recently challenged by novel genetic or pharmacological interferences of BRI1 internalization mechanisms from the cell surface. Blocking BRI1 internalization was shown to activate BR signaling, indicating that BRI1 signals from the plasma membrane [15, 16]. These mechanisms include clathrin-mediated endocytosis, the adaptor complex AP-2 and the ARF-GEFs GNOM and GNL1 [15, 16].

The post-translational modification of proteins by ubiquitination is well-known in yeast and mammals to target proteins to proteasome-mediated degradation. Ubiquitination also serves numerous proteasome-independent roles, including the endocytosis of membrane proteins [17]. In plants, Ub-mediated endocytosis emerged only very recently with the study of ion and hormone transporters [18, 19, 20, 21, 22]. Whether Ub-mediated endocytosis has also been co-opted for driving the trafficking of receptors is unclear. Although several plant E3 ubiquitin ligases have been shown to interact with receptors [23, 24, 25, 26], their direct role in receptor ubiquitination has not been shown. Only the ubiquitination of the cell-surface flagellin receptor FLS2 by the PUB12 and PUB13 E3 ligases targets has been experimentally demonstrated, but linked to proteasomal degradation of FLS2 [27].

Here we demonstrate that BRI1 is post-translationally modified by K63 polyubiquitin chains *in vivo*. Artificial ubiquitination of BRI1 negatively regulates its activity by enhanced vacuolar targeting from EE/TGN and degradation in the vacuole. Mass spectrometry analyses identified residue K866 of BRI1 as a target of ubiquitination *in vivo*. Loss of BRI1

ubiquitination at residue K866 is associated with subtle BR hypersensitivity phenotypes, confirming the negative role played by BRI1 ubiquitination on BR signaling, and pointing to the existence of other ubiquitination sites in BRI1. Model-based prediction of cell surface-exposed lysine residues in BRI1 allowed the generation of a functional but non-ubiquitinatable mutant of BRI1 ($BRI1_{K25R}$). Global loss of BRI1 ubiquitination is associated with major defects in endosomal sorting and vacuolar delivery. Using Total Internal Reflection Fluorescence Microscopy (TIRF-M), we also shed light on the role of BRI1 ubiquitination in the internalization of BRI1 from the cell-surface. In addition, we establish that the control of BRI1 protein dynamics by ubiquitination is a fundamental control mechanism for BR responses in plants. Altogether, our results identify K63-linked polyubiquitin chain formation as a dual targeting signal for BRI1 internalization and sorting along the endocytic pathway, and uncovered its role in hormonally controlled plant development.

Results

BRI1 receptor is ubiquitinated *in vivo*

Earlier work demonstrated that BRI1 undergoes endocytosis and trafficking to the vacuole, independently of its activation state [13]. However, little is known about the mechanisms driving BRI1 protein dynamics in the cell. Ubiquitination of cell-surface receptors in yeast and mammals has been shown to control internalization and/or vacuolar/lysosomal targeting [17]. To determine if BRI1 carries ubiquitin moieties *in vivo*, we used anti-GFP antibodies to immunopreciptate BRI1 from *bri1* mutants complemented by the expression of the functional BRI1::BRI1-mCitrine protein [28]. Similar experiments were performed in parallel in wild-type backgrounds as controls. Immunoprecipitates from BRI1-mCitrine-expressing plants were enriched in BRI1-mCitrine, as attested by the strong signal observed at the expected size of BRI1-mCitrine fusion protein (~170 kDa; Fig. 1a, left panel). To evaluate if a fraction of BRI1 is post-translationally modified by ubiquitination, immunoprecipitates were probed with the general P4D1 anti-Ubiquitin antibodies that recognizes monoubiquitin and several forms of polyubiquitin chains. A high molecular weight smear, typical of ubiquitinated proteins, was specifically observed from ~170kDa in immunoprecipitates from BRI1::BRI1-mCitrine plants (Fig.1a, middle panel). A comparable high molecular weight smear was observed when using the Apu3 K63 polyubiquitin chain-specific antibody, indicating that BRI1 is decorated by K63 polyubiquitin chains *in vivo* (Fig. 1a, right panel).

We next addressed whether ubiquitination of BRI1 was regulated by steroid hormone perception. Challenging plants for 1 hour with 1μM brassinolide (BL), the most active brassinosteroid form, to BRI1-mCitrine plants had no detectable effect on the ubiquitination profile of BRI1-mCitrine (Fig. 1b). It is possible that such young growing BRI1-mCitrine plants have close to maximal levels of activated receptors, thus preventing the detection of ligand-dependent changes in BRI1 ubiquitination. However, two lines of evidence argue against this hypothesis. First, BRI1-mCitrine plants are fully responsive to exogenously applied BL, as observed by the marked change in BES1 phosphorylation status (Fig. S1a), indicating that BR responses are not saturated. Second, growing plants on the BR

biosynthetic inhibitor brassinazole (BRZ) prior to BL treatment had minor effect on BRI1 ubiquitination (Fig. S1b). These observations contrast with the dramatic ubiquitination underwent by the mammalian Epidermal Growth Factor Receptor (EGFR) upon few minutes of EGF exposure [29], a typical example of ligand-induced receptor ubiquitination. Taken together, these observations indicate that BRI1 ubiquitination is largely not regulated by ligand binding to the receptor. They also concur perfectly with the earlier findings that BRI1 trafficking and degradation are ligand-independent [13].

Mechanism of BRI1 ubiquitination

We next investigated the molecular mechanisms driving BRI1 ubiquitination. In particular, we focused on the possible role played by receptor activation, although BRI1 ubiquitination appears to be independent of ligand binding (Fig. 1b). Lysine residue K911 of BRI1 is an invariant residue in subdomain II of kinases and is critical for BRI1 kinase activity and BR signaling. Consequently, *bri1* mutant expressing the kinase-dead K911R mutation are not complemented and show extreme dwarfism [30]. Transgenic plants expressing the non-functional $BRI1_{K911R}$ mutant form under the control of *BRI1* promoter were assayed for BRI1 ubiquitination. In contrast to what is observed in the wild-type form of BRI1, $BRI1_{K911R}$-expressing plants showed reduced ubiquitination (Fig. 1c). This suggests that BRI1 kinase activity is required for ubiquitination. The possibility that residue K911 itself is a major ubiquitination site in BRI1 protein is very unlikely since it is not surface-exposed (Fig. S4a). Mutation in K911 of BRI1 was showed to drastically affect BRI1-BAK1 receptor complex formation [31]. We therefore addressed whether the co-receptor BAK1 was required for BRI1 ubiquitination. To this purpose, we expressed BRI1::BRI1-mCitrine in a *bak1* null mutant background. Compared to wild-type BRI1::BRI1-mCitrine plants, *bak1-3*/BRI1::BRI1-mCitrine showed a reduction in BRI1 ubiquitination (Fig. 1c). Altogether, these results indicate that although BRI1 ubiquitination is not stimulated by steroid perception, it is dependent on BRI1 kinase activity and its co-receptor BAK1, two hallmarks of ligand perception by BRI1 [1].

Artificial ubiquitination of BRI1 triggers rapid endocytosis and vacuolar targeting

Extensive work in yeast and mammals demonstrated the importance of K63 polyubiquitination for plasma membrane protein internalization, and sorting in multivesicular bodies [32]. However, K63 polyubiquitination has also been involved in the regulation of kinases. TAK1 (transforming growth factor-β activating kinase 1) mediates NF-κB activation in response to the activation of TGF-β receptor. Upon stimulation with TGF-β, TAK1 undergoes TRAF6-dependent K63-linked ubiquitination on residue K34. Modification of TAK1 by ubiquitination is critical for TAK1 autophosphorylation and subsequent activation [33]. To get a first glimpse into the biological role of BRI1 post-translational modification by K63 polyubiquitination, we took a gain-of-function approach where BRI1-mCitrine was translationally fused to Ub. We used the complementation of the dwarfism of *bri1* null mutant as readout for BRI1 activity (Fig. S2a). As controls, we also generated *bri1*/BRI1-mCitrine, as well as *bri1*/BRI1-mCitrine-Ub_{I44A} carrying a point mutation in a hydrophobic patch necessary for recognition by ubiquitin-binding domain proteins [34]. Both *bri1*/BRI1-mCitrine and *bri1*/BRI1-mCitrine-$Ub_{I44A,}$ expressing a non-functional ubiquitin, fully complemented the severe dwarfism of *bri1* null mutant (Fig. 2a).

In contrast, BRI1::BRI1-mCitrine-Ub hardly complemented *bri1* phenotype, indicating that artificial ubiquitination of BRI1 down-regulates its activity. Care was taken at that stage to use transgenic lines expressing similar amounts of RNA for the transgene (Fig. S2b). Artificial ubiquitination of BRI1-mCitrine protein led to a strong decrease in total BRI1-mCitrine protein levels compared to wild-type BRI1-mCitrine and BRI1-mCitrine-Ub_{I44A} (Fig. 2b). This is consistent with confocal microscopy observations where BRI1-mCitrine-Ub failed to accumulate with the same detection settings used for BRI1-mCitrine (Fig. 2c). Higher laser intensity and gain however revealed a punctate pattern for BRI1-mCitrine-Ub, with little or no accumulation at the plasma membrane (Fig. 2c inset). These observations indicate that ubiquitination of BRI1 is sufficient to trigger its degradation.

To investigate deeper the mechanisms driving the loss of BRI1-mCitrine-Ub protein, we took advantage of drugs interfering with vesicular trafficking. The fungal toxin Brefeldin A (BFA) is a widely used inhibitor of endosomal trafficking, creating large aggregates of *trans*-Golgi network/early endosomal compartments. Although BRI1-mCitrine-Ub failed to accumulate under normal conditions, BRI1-mCitrine-Ub levels rapidly built up in BFA bodies after BFA treatment (Fig. 2d). This suggests that BRI1-mCitrine-Ub exits the endoplasmic reticulum and passes though the TGN/EE on its way to degradation. We next assessed the influence of the vacuolar ATPase inhibitor Concanamycin A (ConA), which prevents the degradation of proteins targeted to the vacuole. ConA treatment led to the dramatic accumulation of BRI1-mCitrine-Ub in the vacuole (Fig. 2d), compared to BRI1-mCitrine, thus revealing enhanced vacuolar delivery triggered by ubiquitin. This indicates that artificial ubiquitination of BRI1-mCitrine is sufficient for vacuolar targeting.

We next investigated whether BRI1-mCitrine-Ub was trafficking *via* the plasma membrane on its way to the vacuole by inhibiting clathrin-mediated endocytosis, the major endocytic road in plants [35]. TyrA23 treatment was ineffective at stabilizing BRI1-mCitrine-Ub at the cell surface, but rather led to a cytosolic-like pattern of fluorescence (Fig. S2c). In contrast, TyrA23 prevented the formation of BFA bodies in BRI1-mCitrine plants (Fig. S2d), attesting that TyrA23 treatment was active. Taken together, these results indicate that artificial ubiquitination is recognized at the TGN/EE and serves as a targeting signal for degradation in the vacuole.

BRI1 is ubiquitinated at residue K866 *in vivo*

To identify ubiquitination sites in BRI1, we performed immunoprecipitation of BRI1 in the presence of deubiquitinase inhibitors followed by mass spectrometry analyses. Immunopurified BRI1-mCitrine was digested by trypsin and subjected to liquid-chromatography tandem mass spectrometry analyses (LC-MS/MS). Multidimensional Protein Identification Technology (MudPIT) analyses on BRI1-mCitrine immunoprecipitates detected 9 BRI1 peptides, including the EALSINLAAFEK^{GG}PLR peptide modified by the tryptic ubiquitin remnant G-G isopeptide on the lysine residue K866. This residue lies on the cytosolic face of BRI1 protein, in the juxtamembrane domain (Fig. 3a). To examine the biological role of K866 ubiquitination, we generated the *bri1*/BRI1::$BRI1_{K866R}$-mCitrine where K866 is substituted to the positively charged but non-ubiquitinatable R residue. *bri1*/BRI1::$BRI1_{K866R}$-mCitrine transgenic plants expressing

similar BRI1-mCitrine levels than *bri1*/BRI1::BRI1-mCitrine possessed slightly more dephosphorylated BES1 (Fig. 3b), a hallmark of active BR signaling. Although *bri1*/BRI1::$BRI1_{K866R}$-mCitrine plants displayed a wild-type phenotype at the rosette stage (Fig. 3c), such plants showed slightly longer hypocotyls when grown under both normal conditions and BRZ (Fig. 3d). This latter observation is consistent with BRI1 ubiquitination being largely independent on the ligand (Fig. 1b). No striking difference on the localization and the levels of $BRI1_{K866R}$-mCitrine protein could be observed, however (Fig. 3e). Altogether, ubiquitination of residue K866 appears to play a negative role on BRI1 activity. Nevertheless, it is clear from the mild BR-related phenotypes displayed by *bri1*/BRI1::$BRI1_{K866R}$-mCitrine transgenic plants, and from its ubiquitination profile still harboring massive ubiquitination (Fig. S3), that many more ubiquitination sites are expected in BRI1 protein.

Loss of BRI1 ubiquitination impairs both internalization and vacuolar targeting

The intracellular domain of BRI1 contains 29 lysine residues. Sequence alignment of BRI1 with i) the BRLs BRI1 homologs from Arabidopsis, ii) BRI1 from other species, iii) Arabidopsis receptor kinases belonging to different subfamilies (FLS2, CLV1) and iv) human IRAK4 indicate that four lysines are highly conserved in BRI1 kinase. These include the ATP-binding pocket-located K899, K911 and K912, and residue K1011 in the catalytic loop. Model prediction for BRI1 kinase domain, based on the structure of hsIRAK4 indicates that most other lysine residues are either surface exposed or close to the surface and potentially accessible for post-translational modification (Fig. S4a). To pinpoint the role of BRI1 ubiquitination, we mutated 25 lysines to arginines and conserved only the four conserved lysine residues required for kinase activity. Strikingly, expression of the resulting $BRI1_{K25R}$ mutants complemented the dwarf phenotype of *bri1* null mutant (Fig. 4a). This result indicates that $BRI1_{K25R}$-mCitrine was still functional and that none of these 25 lysines are required for receptor activation. However, $BRI1_{K25R}$-mCitrine ubiquitination was reduced compared to BRI1-mCitrine (Fig. S4b). Interestingly, $BRI1_{K25R}$-expressing plants showed long bending petioles and narrow leaf blades (Fig. 4b), reminiscent of what is observed in BRI1-overexpressors [36]. The BR hypersensitivity phenotype of $BRI1_{K25R}$ is observed even when plants express less BRI1 proteins than *bri1*/BRI1-mCitrine plants (Fig. 4c), highlighting further the negative role played by ubiquitination on BRI1 activity.

BRI1 protein is found under normal conditions at the plasma membrane, but also in endosomal compartments (TGN/EE and MVB) (Fig. 4d) [13, 14]. In contrast, $BRI1_{K25R}$-mCitrine was found mostly at the cell-surface with little intracellular compartments observed. To unravel the mechanism leading to more $BRI1_{K25R}$-mCitrine being found at the plasma membrane, we compared the endocytic trafficking of BRI1-mCitrine and $BRI1_{K25R}$-mCitrine. BFA inhibits the trafficking of membrane proteins from TGN/EEs to MVBs and recycling to the plasma membrane, but allows endocytosis. Both BRI1-mCitrine and $BRI1_{K25R}$-mCitrine accumulated in BFA compartments in absence of *de novo* protein synthesis (Fig. 4e). This suggests that $BRI1_{K25R}$-mCitrine still underwent internalization from the plasma membrane. To obtain more resolution and quantitative data on the dynamics of BRI1 and $BRI1_{K25R}$ at the cell surface, we implemented Total Internal Reflection Fluorescence microscopy (TIRF). TIRF generates high contrast images and

allows studying the dynamic behavior of proteins at the plasma membrane. BRI1-mCitrine-expressing plants were imaged by TIRF microscopy over time and showed small diffraction-limited fluorescent spots (Movie S1, S2). These spots were immobile on the (x,y) axis but dynamically appeared and disappeared from the focal plane, thus representing fusion and fission events at the cell surface. A similar pattern was observed for $BRI1_{K25R}$-mCitrine, although the density of spots at the cell surface was higher (Fig. S4c). To grasp the role of ubiquitination in BRI1 internalization from the plasma membrane, we further analyzed the dynamic behavior of wild-type BRI1 and $BRI1_{K25R}$ by kymograph analysis. Kymographs monitor on a single image the intensity at a given (x,y) location over time, and allow determination of surface time residence for wild-type BRI1 and its non-ubiquitinatable counterpart by measuring track length (Fig. 4f). The time of residency of BRI1-mCitrine at the cell surface was widely distributed (Fig. 4g), but over 60% of the spots resided less than 10s at the plasma membrane. The distribution observed for $BRI1_{K25R}$ was markedly different, with most spots persisting longer at the plasma membrane. The surface residence time median values for BRI1 and $BRI1_{K25R}$ were 7.2s and 28.6s, respectively (Fig. S4d). These observations clearly argue for a direct role of BRI1 ubiquitination in internalization of the plasma membrane.

We next monitored the role of ubiquitination in BRI1 vacuolar targeting. BRI1-mCitrine and $BRI1_{K25R}$-mCitrine were transferred to dark conditions, which impair vacuolar lytic activity and allow visualization of fluorescent fusion proteins targeted to the vacuole, and monitored by confocal microscopy. Consistently, BRI1-mCitrine showed vacuolar accumulation after 2 hours of darkness (Fig. 4h). However, $BRI1_{K25R}$-mCitrine exhibited no vacuolar targeting within the same time frame. Altogether, our results demonstrate that BRI1 ubiquitination plays a role in BRI1 receptor internalization from the plasma membrane and also acts on its endosomal sorting and vacuolar targeting.

Discussion

The BR receptor BRI1 is the best-studied plant receptor and serves as the archetypical receptor to study the activation/deactivation mechanisms involved in receptor-mediated signaling. Previous studies have shed light on the ligand-dependent oligomerization and phosphorylation of the BRI1/BAK1 receptor complex and have identified components of the BR signaling pathway controlling BR genomic responses [37]. However, not much is known about the mechanisms driving the trafficking of BRI1 and its turnover in relationship with signaling. In this report, we show that BRI1 dynamics in the cell is controlled by K63 polyubiquitination and unravel its crucial role for BR-mediated plant growth.

Ubiquitination of proteins has been associated with many different cellular outputs in yeast and mammals, depending on the type of ubiquitination [32]. In the case of membrane proteins, ubiquitination triggers endocytosis and vacuolar/lysosomal degradation [17]. In plants, only a handful of integral membrane proteins have been shown to undergo Ub-mediated endocytosis. These examples are so far exclusively restricted to multispan transporters involved in iron, boron or phosphate nutrition or in auxin transport [18, 19, 20, 21]. Both monoubiquitination and K63 polyubqiuitination has been implicated in these examples, consistent with their described roles in yeast and mammals. Ubiquitination of plant receptors

is still poorly documented, although several E3-Ub ligases interacting with receptors have been identified [23, 24, 25, 26]. The Flagellin receptor FLS2 involved in plant immune responses have been shown to be ubiquitinated by K48 polyubiquitin chains and degraded by the proteasome [27]. Using a gain-of-function approach, we demonstrated that the artificial ubiquitination of BRI1 is sufficient for destabilizing the corresponding protein (Fig. 2a). Destabilization of BRI1-mCitrine-Ub protein involves trafficking through the TGN/EE and degradation in the vacuole, based on the strong accumulation of BRI1-mCitrine-Ub following treatments with BFA and ConcA. Inhibition of clathrin-mediated endocytosis, the major BRI1 endocytic route [15, 16], with TyrA23 failed to stabilize BRI1-mCitrine-Ub at the cell-surface (Fig. S2d), suggesting that the ubiquitinated BRI1 variant never reaches the surface. Formally, artificially ubiquitinated BRI1 could be rapidly endocytosed from the plasma membrane using a clathrin-independent pathway, we favor the hypothesis that BRI1-mCitrine-Ub is recognized at the TGN/EE and diverted away from the secretory pathway before it reaches the plasma membrane, being directly routed to the vacuole for degradation. The sorting and vacuolar/lysosomal targeting of ubiquitinated cargos in yeast and mammals require the late endosome-located ESCRT complex [17]. In plants, several subunits of the ESCRT complex have been detected in TGN/EE [38], indicating that the sorting of ubiquitinated cargos and BRI1-mCitrine indeed occurs already at the TGN/EE. The combination of ubiquitination site identification by mass spectrometry and model-based prediction allowed us to generate a functional ubiquitination-defective $BRI1_{K25R}$ mutant form. In contrast to wild-type BRI1 that shows significant endosomal localization [13], $BRI1_{K25R}$ was mostly found at the cell surface (Fig. 4d). Besides residue K866, BRI1 carries several redundant ubiquitination sites although their precise location is not defined. Detailed analysis of $BRI1_{K25R}$ trafficking revealed its inability to reach the vacuole under dark condition (Fig. 4h), clearly demonstrating that BRI1 ubiquitination plays critical proteasome-independent roles by driving vacuolar targeting. These observations are in accordance with the enhanced vacuolar delivery of artificially ubiquitinated BRI1-mCitrine-Ub (Fig. 2d) and with what has been reported previously for EGFR [39].

The fact that BRI1-mCitrine-Ub is sorting at TGN/EE before reaching the cell-surface prevents us from investigating the role of ubiquitination in internalization of BRI1 from the plasma membrane. To circumvent this limitation, we implemented TIRF microscopy to specifically monitor BRI1 dynamics at the cell surface. Such analysis first highlighted the highly dynamic behavior of wild-type BRI1, with extremely rapid fusion and fission events within the seconds range (Fig. 4f, movies S1, S2). This fast mode of endocytosis and recycling resemble “kiss and run” models in which the vesicle opens and closes transiently, as described for synaptic vesicles [40]. Interestingly, $BRI1_{K25R}$ shows much slower fusion/fission events at the plasma membrane, within the tens of second range (Fig. 4f). Ubiquitination of BRI1 therefore appears as one mechanism of BRI1 internalizing from the plasma membrane, although Ub-independent mechanisms are at stake in contrast to the fundamental role of Ub in endosomal sorting. Slower internalization and recycling caused by the vacuolar targeting defect could be the basis of increased $BRI1_{K25R}$ at the cell surface and increased spot density. This scenario is reminiscent of what is currently debated for the Epidermal Growth Factor Receptor (EGFR) in animals. Inhibition of ubiquitination by mutating 15 ubiquitin conjugation sites found in the EGFR kinase domain or the Cbl E3

ligase-binding site does not affect internalization, although preventing lysosomal degradation [39]. EGFR internalization from the cell surface is impaired only when 21 lysine residues in the kinase domain and C-terminal domain are mutated, although the three distal lysines in the C-terminal domain appeared to be acetylated [41]. EGFR internalization is dependent on many redundant lysine residues and involves several redundant and cooperative mechanisms [41].

Modification of BRI1 with Ub negatively regulates BRI1 function and BR signaling, as attested by the BR-hypersensitive phenotypes displayed by transgenic plants impaired in BRI1 ubiquitination (Fig. 4a, b). BRI1 ubiquitination is however largely independent of ligand binding (Fig. 1b, S1b), consistent with previous observations showing that BRI1 turnover is not modulated by the presence or absence of BRs [13]. Surprisingly, BRI1 ubiquitination required BRI1 kinase activity and the presence of its co-receptor BAK1 (Fig. 1c), both mechanisms being dependent on BRs. One explanation is that in the absence of steroids, BRI1 kinase shows basal kinase activity sufficient for triggering phosphorylation of important residues for ubiquitination in BRI1 or another substrate protein, but not involved in signaling. The requirement for BAK1 is puzzling considering the BR-dependency of BRI1/BAK1 interaction. However, recent evidence based on FRET-FLIM analyses indicates that significant proportion of BRI1 and BAK1 interact at the cell surface even in the absence of ligand [42]. These different observations clarify how BRI1 ubiquitination may rely on hallmarks of BR receptor complex activation, although independently of ligand perception. The ability of BRI1 to signal from endosome has been highly debated recently. The increased plasma membrane localization of $BRI1_{K25R}$ associated to enhanced BR signaling confirms recent evidence pointing to the initiation of BR signaling at the cell surface. BRI1 ubiquitination appears as a mechanism controlling the dynamics of BRI1 in the cell and thus impact on BR signaling, although in a BR-independent manner. Whether endogenous/exogenous cues may impact on BRI1 ubiquitination and thus affect BR-dependent growth will have to be investigated in the future.

Altogether, our work identify K63-linked polyubiquitin chain formation as a dual targeting signal for BRI1 internalization and sorting along the endocytic pathway, and highlight its role in the control of plant development by BR hormones.

Experimental Procedures

Plant material and constructs

Wild-type (Col0), *bak1-3* [43], *bri1* [28] and the various transgenic plants generated in this study were grown at 21 °C with 16-h light/8-h dark cycles.

BRI1::BRI1-mCitrine, *bri1*/BRI1::BRI1-mCitrine, *bak1-3*/BRI1::BRI1-mCitrine and kinase-dead BRI1::$BRI1_{K911R}$-mCitrine were previously characterized [28, 36]

mCitrine-Ub fusion was cloned into pDONR-P2RP3 (Invitrogen). $BRI1_{K866R}$ and $BRI1_{K25R}$ were cloned in pDONR221 (Invitrogen). Final destination vectors were obtained by using three fragments recombination system using the pB7m34GW destination vectors [44], and the entry vectors pDONR-P4P1r-BRI1prom [28], pDONR221-BRI1 or mutated BRI1 versions,

and pDONR-P2rP3-mCitrine [28] or mCitrine-Ub. The constructs were transformed into heterozygous *bri1* null mutant or wild-type plants. For all constructs, more than 20 independent T1 lines were isolated and between 3 to 6 representative mono-insertion lines were selected in T2. Confocal microscopy, phenotypic analysis and protein extraction were performed on segregating T2 and homozygous T3 lines.

Chemical treatments

Inhibitors (Sigma-Aldrich) were used at the following concentrations: 2 μM ConcA (2 mM DMSO stock), 50 μM BFA (50 mM DMSO stock), 33 μM TyrA23 (50 mM DMSO stock), 100μM CHX (100mM EtOH stock). BL (Chemiclones, 1 mM stock in DMSO) and BRZ (Chemiclones, 10 mM stock in DMSO) were used at concentrations indicated in the figure legends.

Hypocotyl and petiole length assays

Hypocotyl and petiole lengths from 15 seedlings were measured with ImageJ 1.48d on day 4 and 28, respectively. All dose-response experiments were performed at least in duplicate.

Immunoprecipitation and Western Blot Analysis

Protein extraction and immunoprecipitation experiments were conducted exactly as described previously (Jaillais et al., 2011). For protein detection, the following antibodies were used: Monoclonal anti-GFP HRP-coupled (Miltenyi Biotech), anti-ubiquitin P4D1 (Millipore), anti-K63 polyubiquitin Apu3 (Millipore) and anti-BES1 (Yu et al., 2011). Quantification of western blot was performed using the Densitometry plugin from Image J 1.48d.

Mass Spectrometry

Immunopurified proteins were reduced with DTT, alkylated with iodoacetamide and digested with trypsin overnight. Salts and reagents were removed by reversed phase (C-18) cartridge clean-up. The salt-free peptides were dissolved in 0.1% formic acid and subjected to ESI-MS/MS analysis on a Thermo LTQ-Orbitrap XL instrument. A capillary column (inner diameter 75 μm, packing length 10 cm of C-18 silica) with integrated spray tip was used with a 300 nl/min 0.1% formic acid/acetonitrile gradient. Peptide precursor masses were determined with high accuracy by Fourier-transform MS in the Orbitrap followed by data dependent MS/MS of the top 5 precursor ions in each chromatographic time window. Data were analyzed using the Mascot algorithm (Matrix Science, London, (UK) on a local Mascot server (version 2.1.0) and searched against the latest Swiss Protein database allowing a variable isopeptide (Gly-Gly) modification on lysine residues.

Model prediction

The kinase domain of BRI1 (residues 867 à 1158) was modeled using the software SWISS-MODEL (http://swissmodel.expasy.org/) and the interleukin-1 (IL-1) receptor-associated kinase-4 (IRAK-4) as template (PDB code 2NRU).

Confocal microscopy

Plant samples were mounted in water and viewed on Leica TCS SP2 confocal laser scanning microscopes. For imaging mCitrine fusion proteins, the 514-nm laser line was used. Laser intensity settings were kept constant in individual sets of experiments to allow for a comparison of expression and localization of reporter proteins.

TIRF microscopy and analysis of images

Arabidopsis plantlets were grown in MS medium for 5 days in the dark to obtain etiolated hypocotyls. Hypocotyls were imaged by TIRF on a Nikon Eclipse Ti microscope equipped with a Nikon APO TIRF 100×/1.49 oil immersion objective. The excitation wavelength used was 491 nm provided by a 100 mW diode laser Toptica AOTF and emission light was collected with an emission filter Chroma ET 525/50. Time-lapses were acquired during 2 minutes at 200 ms intervals and images were captured with a Photometrics® Evolve Delta Camera using the Metamorph Software version 7.7.9.0 (Molecular Devices®, LLC) and the laser power at 40%. The videos of 3 independent experiments were then analyzed using the ImageJ 1.48d software. To better visualize the videos, the Difference of Gaussian filter and the kymographs were obtained on the treated images using the MultiKymographs plugin (http://www.embl.de/eamnet/html/body_kymograph.html) of ImageJ. The time of residence was determined by the duration of tracks (n=350). To measure the density of BRI1 and $BRI1_{K25R}$ at the plasma membrane, videos were treated with the Difference of Gaussian filter and the density of protein was quantified by the Find Maxima function within a region of same area using ROI manager. Each area measured was 40×41 pixels (0.160μm/pixel) in size.

Acknowledgements

We thank the IMAGIF Imaging facility for TIRF analyses and Arthur Molines for help with image analyses. S.M is sponsored by a PhD fellowship from the Saclay Plant Sciences LabEx initiative (ANR-10-LABX-0040-SPS) funded by the French government and the Agence Nationale de la Recherche (ANR-11-IDEX-0003-02), and E.M.N.D. by an EMBO long-term fellowship. This work was supported by a grant from the National Institutes of Health (5 R01 GM094428), the Howard H. and Maryam R. Newman Chair in Plant Biology, and the Howard Hughes Medical Institute (to J.C.), a grant from the Swiss National Science Foundation (31003A_120558) (to N.G.), grants from Marie Curie Action (PCIG-GA-2012-334021) and Agence Nationale de la Recherche (to G.V).

References

1. Vert G, Nemhauser JL, Geldner N, Hong F, Chory J. Molecular mechanisms of steroid hormone signaling in plants. Annu Rev Cell Dev Biol. 2005; 21:177–201. [PubMed: 16212492]
2. Fridman Y, Savaldi-Goldstein S. Brassinosteroids in growth control: how, when and where. Plant Sci. 2013; 209:24–31. [PubMed: 23759100]
3. Hothorn M, et al. Structural basis of steroid hormone perception by the receptor kinase BRI1. Nature. 2011; 474:467–471. [PubMed: 21666665]
4. Santiago J, Henzler C, Hothorn M. Molecular mechanism for plant steroid receptor activation by somatic embryogenesis co-receptor kinases. Science. 2013; 341:889–892. [PubMed: 23929946]
5. She J, et al. Structural insight into brassinosteroid perception by BRI1. Nature. 2011; 474:472–476. [PubMed: 21666666]
6. Kim TW, et al. Brassinosteroid signal transduction from cell-surface receptor kinases to nuclear transcription factors. Nat Cell Biol. 2009; 11:1254–1260. [PubMed: 19734888]
7. Tang W, et al. PP2A activates brassinosteroid-responsive gene expression and plant growth by dephosphorylating BZR1. Nat Cell Biol. 2011; 13:124–131. [PubMed: 21258370]

8. He JX, et al. BZR1 is a transcriptional repressor with dual roles in brassinosteroid homeostasis and growth responses. Science. 2005; 307:1634–1638. [PubMed: 15681342]
9. Yin Y, Vafeados D, Tao Y, Yoshida S, Asami T, Chory J. A new class of transcription factors mediates brassinosteroid-regulated gene expression in Arabidopsis. Cell. 2005; 120:249–259. [PubMed: 15680330]
10. Sun Y, et al. Integration of brassinosteroid signal transduction with the transcription network for plant growth regulation in Arabidopsis. Dev Cell. 2010; 19:765–777. [PubMed: 21074725]
11. Vert G, Chory J. Downstream nuclear events in brassinosteroid signalling. Nature. 2006; 441:96–100. [PubMed: 16672972]
12. Yu X, et al. A brassinosteroid transcriptional network revealed by genome-wide identification of BESI target genes in Arabidopsis thaliana. Plant J. 2011; 65:634–646. [PubMed: 21214652]
13. Geldner N, Hyman DL, Wang X, Schumacher K, Chory J. Endosomal signaling of plant steroid receptor kinase BRI1. Genes Dev. 2007; 21:1598–1602. [PubMed: 17578906]
14. Jaillais Y, Fobis-Loisy I, Miege C, Gaude T. Evidence for a sorting endosome in Arabidopsis root cells. Plant Journal. 2008; 53:237–247. [PubMed: 17999644]
15. Di Rubbo S, et al. The clathrin adaptor complex AP-2 mediates endocytosis of brassinosteroid insensitive1 in Arabidopsis. Plant Cell. 2013; 25:2986–2997. [PubMed: 23975899]
16. Irani NG, et al. Fluorescent castasterone reveals BRI1 signaling from the plasma membrane. Nat Chem Biol. 2012; 8:583–589. [PubMed: 22561410]
17. MacGurn JA, Hsu PC, Emr SD. Ubiquitin and membrane protein turnover: from cradle to grave. Annu Rev Biochem. 2012; 81:231–259. [PubMed: 22404628]
18. Barberon M, et al. Monoubiquitin-dependent endocytosis of the iron-regulated transporter 1 (IRT1) transporter controls iron uptake in plants. Proc Natl Acad Sci U S A. 2011; 108:E450–458. [PubMed: 21628566]
19. Kasai K, Takano J, Miwa K, Toyoda A, Fujiwara T. High boron-induced ubiquitination regulates vacuolar sorting of the BOR1 borate transporter in Arabidopsis thaliana. J Biol Chem. 2011; 286:6175–6183. [PubMed: 21148314]
20. Leitner J, et al. Lysine63-linked ubiquitylation of PIN2 auxin carrier protein governs hormonally controlled adaptation of Arabidopsis root growth. Proc Natl Acad Sci U S A. 2012; 109:8322–8327. [PubMed: 22556266]
21. Lin WY, Huang TK, Chiou TJ. NITROGEN LIMITATION ADAPTATION, a Target of MicroRNA827, Mediates Degradation of Plasma Membrane-Localized Phosphate Transporters to Maintain Phosphate Homeostasis in Arabidopsis. Plant Cell. 2013; 25:4061–4074. [PubMed: 24122828]
22. Shin L-J, Lo J-C, Chen G-H, Callis J, Fu H, Yeh K-C. IRT1 DEGRADATION FACTOR1, a RING E3 Ubiquitin Ligase, Regulates the Degradation of IRON-REGULATED TRANSPORTER1 in Arabidopsis. Plant Cell. 2013; 25:3039–3051. [PubMed: 23995086]
23. Gu T, Mazzurco M, Sulaman W, Matias DD, Goring DR. Binding of an arm repeat protein to the kinase domain of the S-locus receptor kinase. Proc Natl Acad Sci U S A. 1998; 95:382–387. [PubMed: 9419384]
24. Kim M, Cho HS, Kim DM, Lee JH, Pai HS. CHRK1, a chitinase-related receptor-like kinase, interacts with NtPUB4, an armadillo repeat protein, in tobacco. Biochim Biophys Acta. 2003; 1651:50–59. [PubMed: 14499588]
25. Samuel MA, et al. Interactions between the S-domain receptor kinases and AtPUB-ARM E3 ubiquitin ligases suggest a conserved signaling pathway in Arabidopsis. Plant Physiol. 2008; 147:2084–2095. [PubMed: 18552232]
26. Wang YS, et al. Rice XA21 binding protein 3 is a ubiquitin ligase required for full Xa21- mediated disease resistance. Plant Cell. 2006; 18:3635–3646. [PubMed: 17172358]
27. Lu D, et al. Direct ubiquitination of pattern recognition receptor FLS2 attenuates plant innate immunity. Science. 2011; 332:1439–1442. [PubMed: 21680842]
28. Jaillais Y, Belkhadir Y, Balsem√£o-Pires E, Dangl JL, Chory J. Extracellular leucine-rich repeats as a platform for receptor/coreceptor complex formation. Proceedings of the National Academy of Sciences. 2011; 108:8503–8507.

29. de Melker AA, van der Horst G, Calafat J, Jansen H, Borst J. c-Cbl ubiquitinates the EGF receptor at the plasma membrane and remains receptor associated throughout the endocytic route. J Cell Sci. 2001; 114:2167–2178. [PubMed: 11493652]
30. Wang X, et al. Identification and functional analysis of in vivo phosphorylation sites of the Arabidopsis BRASSINOSTEROID-INSENSITIVE1 receptor kinase. Plant Cell. 2005; 17:1685–1703. [PubMed: 15894717]
31. Wang X, et al. Sequential transphosphorylation of the BRI1/BAK1 receptor kinase complex impacts early events in brassinosteroid signaling. Dev Cell. 2008; 15:220–235. [PubMed: 18694562]
32. Mukhopadhyay D, Riezman H. Proteasome-independent functions of ubiquitin in endocytosis and signaling. Science. 2007; 315:201–205. [PubMed: 17218518]
33. Sorrentino A, et al. The type I TGF-beta receptor engages TRAF6 to activate TAK1 in a receptor kinase-independent manner. Nat Cell Biol. 2008; 10:1199–1207. [PubMed: 18758450]
34. Hicke L, Schubert HL, Hill CP. Ubiquitin-binding domains. Nat Rev Mol Cell Biol. 2005; 6:610–621. [PubMed: 16064137]
35. Dhonukshe P, et al. Clathrin-mediated constitutive endocytosis of PIN auxin efflux carriers in Arabidopsis. Curr Biol. 2007; 17:520–527. [PubMed: 17306539]
36. Belkhadir Y, Jaillais Y, Epple P, Balsemao-Pires E, Dangl JL, Chory J. Brassinosteroids modulate the efficiency of plant immune responses to microbe-associated molecular patterns. Proc Natl Acad Sci U S A. 2012; 109:297–302. [PubMed: 22087001]
37. Zhu JY, Sae-Seaw J, Wang ZY. Brassinosteroid signalling. Development. 2013; 140:1615–1620. [PubMed: 23533170]
38. Scheuring D, et al. Multivesicular bodies mature from the trans-Golgi network/early endosome in Arabidopsis. Plant Cell. 2011; 23:3463–3481. [PubMed: 21934143]
39. Huang F, Goh LK, Sorkin A. EGF receptor ubiquitination is not necessary for its internalization. Proc Natl Acad Sci U S A. 2007; 104:16904–16909. [PubMed: 17940017]
40. Rizzoli SO, Jahn R. Kiss-and-run, collapse and 'readily retrievable' vesicles. Traffic. 2007; 8:1137–1144. [PubMed: 17645434]
41. Goh LK, Huang F, Kim W, Gygi S, Sorkin A. Multiple mechanisms collectively regulate clathrin-mediated endocytosis of the epidermal growth factor receptor. J Cell Biol. 2010; 189:871–883. [PubMed: 20513767]
42. Bucherl CA, et al. Visualization of BRI1 and BAK1(SERK3) membrane receptor heterooligomers during brassinosteroid signaling. Plant Physiol. 2013; 162:1911–1925. [PubMed: 23796795]
43. Chinchilla D, et al. A flagellin-induced complex of the receptor FLS2 and BAK1 initiates plant defence. Nature. 2007; 448:497–500. [PubMed: 17625569]
44. Karimi M, Depicker A, Hilson P. Recombinational cloning with plant gateway vectors. Plant Physiol. 2007; 145:1144–1154. [PubMed: 18056864]

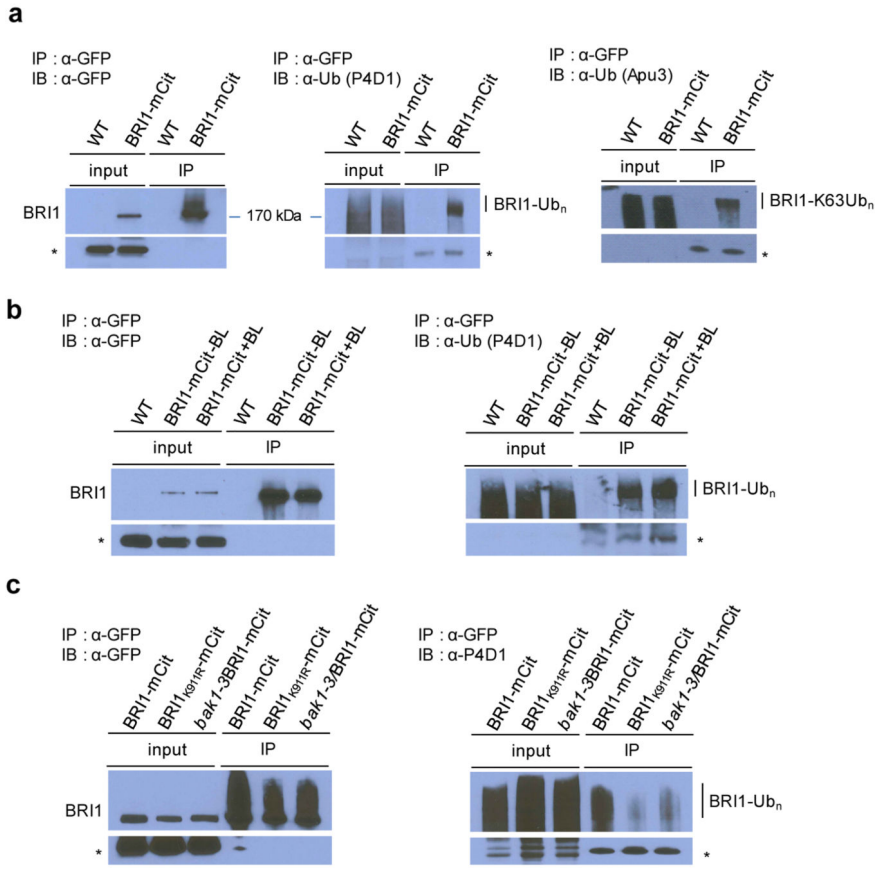

Figure 1. BRI1 carries K63 polyubiquitin chains *in vivo*, independently of ligand binding

(**a**) *In vivo* ubiquitination analyses of BRI1. Immunoprecipitation was performed using an anti-GFP antibody on solubilized protein extracts from wild-type and BRI1-mCitrine plants and subjected to immunoblotting with anti-GFP (left), anti-Ub P4D1 (middle) and anti-K63 polyUb Apu3 (right) antibodies. IB, immunoblotting; IP, immunoprecipitation. (**b**) Ligand-dependency of BRI1 ubiquitination. Ubiquitination assays were performed on wild-type and BRI1-mCitrine plants treated with mock (−BL) or 1μM BL (+BL) for 1 hour. (**C**) BRI1 ubiquitination in mutants affected in receptor complex activation. Ubiquitination assays were performed on BRI1-mCitrine, kinase-dead BRI1$_{K911R}$-mCitrine, and *bak1-3*/BRI1-mCitrine plants. The asterisk indicates aspecific signals used as loading control. See also Figure S1.

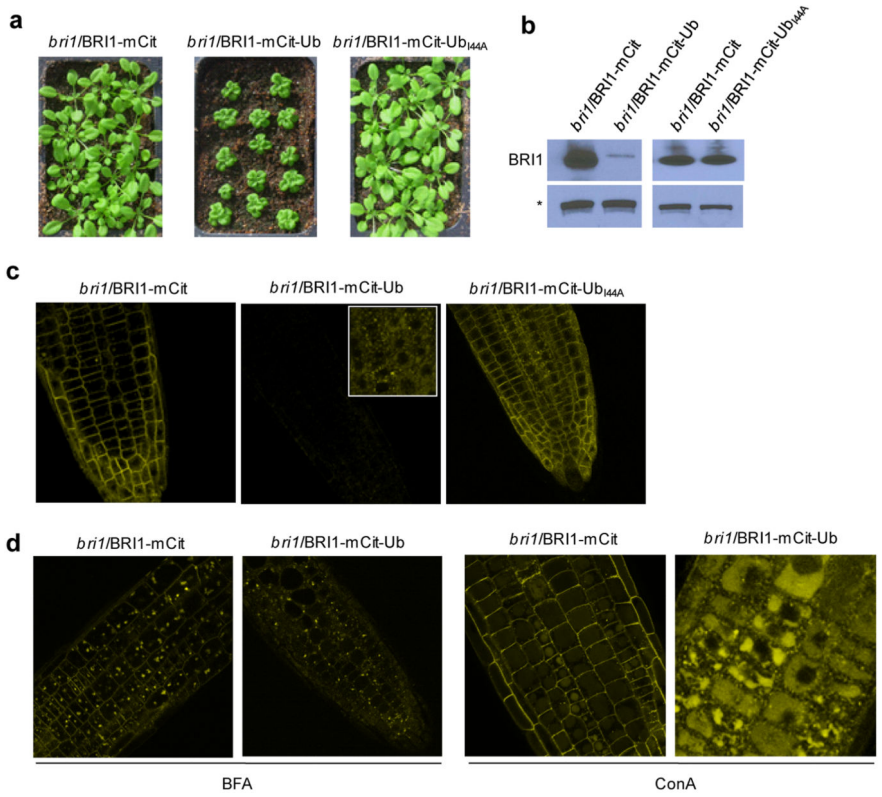

Figure 2. Artificial ubiquitination of BRI1 triggers vacuolar targeting from TGN/EE

(**a**) Phenotypic analysis of transgenic plants expressing BRI1-mCitrine, BRI1-mCitrine-Ub and BRI1-mCitrine-Ub_{I44A} in the *bri1* null background. (**b**) Western blot analyses of BRI1 protein accumulation in *bri1*/BRI1-mCitrine, *bri1*/BRI1-mCitrine-Ub and *bri1*/BRI1-mCitrine-Ub_{I44A} plants using an anti-GFP antibody. The asterisk indicates aspecific signals used as loading control. (**c**) Confocal microscopy analyses of *bri1*/BRI1-mCitrine, *bri1*/BRI1-mCitrine-Ub and *bri1*/BRI1-mCitrine-Ub_{I44A} roots. Similar detection settings were used to compare the different lines. Inset, higher laser power and gain. (**d**) Drug sensitivity of *bri1*/BRI1-mCitrine and *bri1*/BRI1-mCitrine-Ub plants. Plants were exposed to BFA (50μM) and ConcA (2μM) for 30 minutes and 1 hour, respectively. Similar detection settings were used to compare the different lines. See also Figure S2.

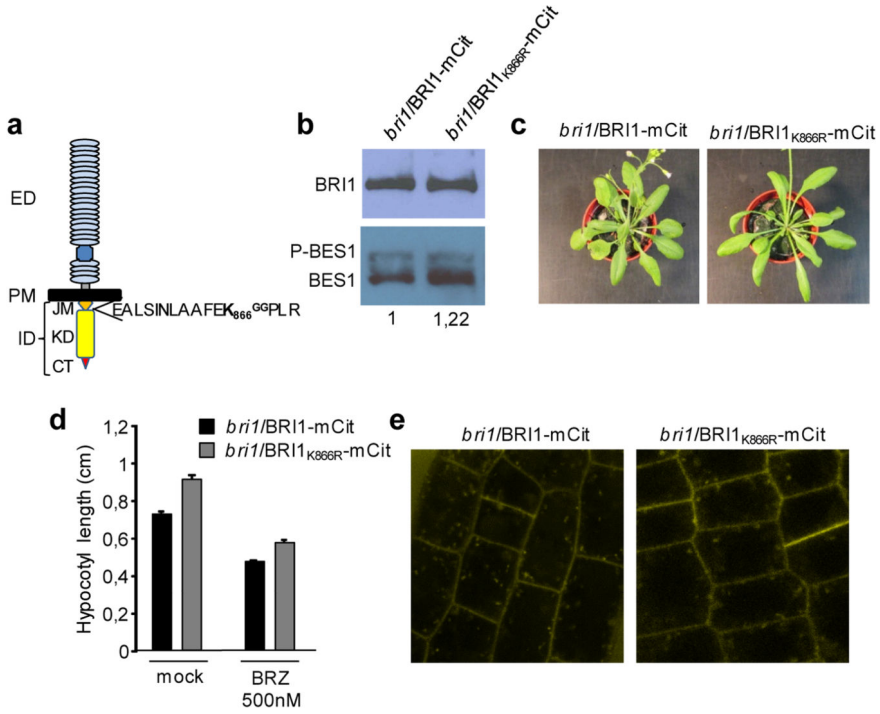

Figure 3. Ubiquitination of residue K866 negatively regulates BRI1

(**a**) Identification of *in vivo* ubiquitination sites in BRI1. ED, extracellular domain; PM, plasma membrane, ID, intracellular domain; JM, juxtamembrane domain; KD, kinase domain; CT, C-terminal domain. The ubiquitinated peptide carrying the GG signature on K866 is shown. (**b**) Western blot analyses on *bri1*/BRI1-mCitrine and *bri1*/BRI1$_{K866R}$-mCitrine plants. Protein levels were detected with anti-GFP and anti-BES1 antibodies, respectively. Quantification of dephosphorylated BES1 protein, normalized to BRI1 levels is shown. (**c**) Phenotypic analysis of 4-week-old *bri1*/BRI1-mCitrine and *bri1*/BRI1$_{K866R}$-mCitrine plants. (**d**) Average hypocotyl lengths of 3-day-old etiolated *bri1*/BRI1-mCitrine and *bri1*/BRI1$_{K866R}$-mCitrine seedlings (n=15). Error bars indicate standard deviation. (**e**) Confocal microscopy analyses of *bri1*/BRI1-mCitrine and *bri1*/BRI1$_{K866R}$-mCitrine roots. See also Figure S3.

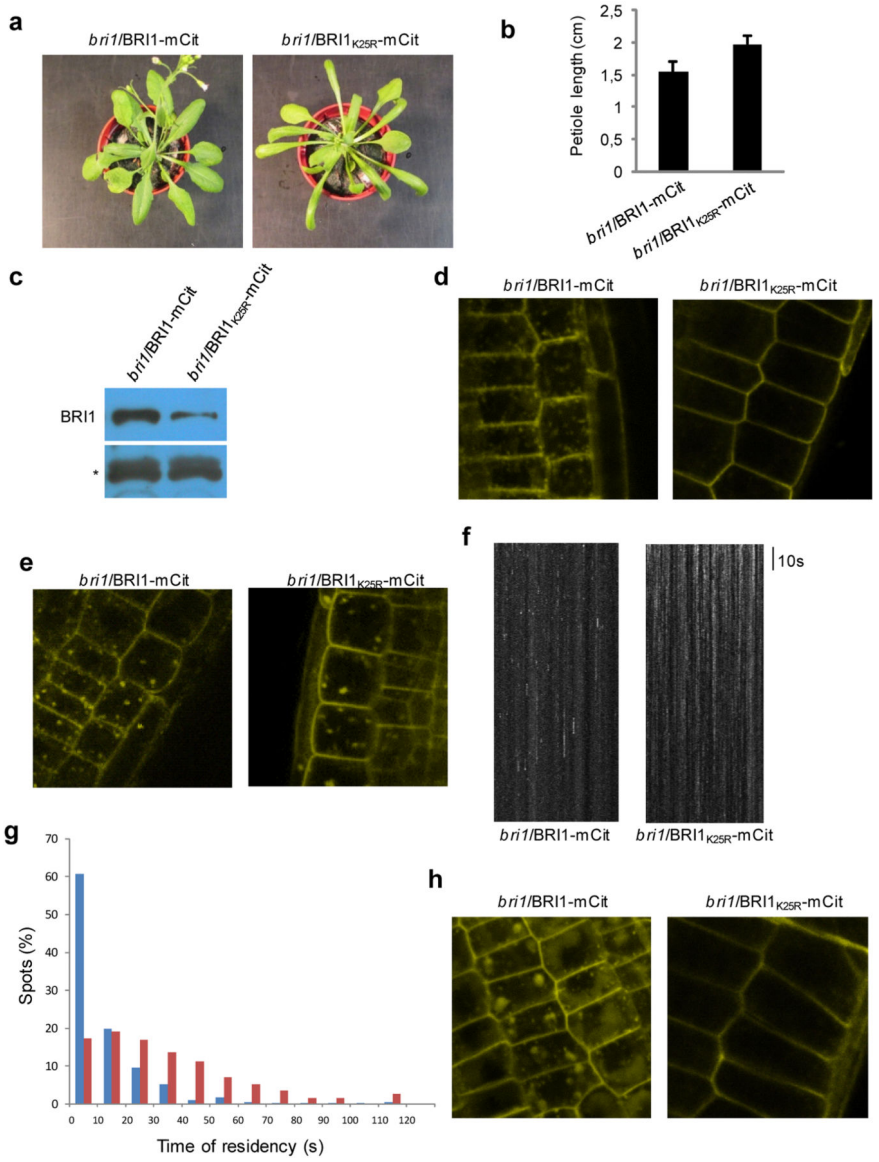

Figure 4. Loss of BRI1 ubiquitination impairs internalization and vacuolar targeting

(**a**) Phenotypic analysis of 4-week-old *bri1*/BRI1-mCitrine and *bri1*/BRI1$_{K25R}$-mCitrine plants. (**b**) Average petiole lengths of the fourth true leaf from of 4-week-old *bri1*/BRI1-mCitrine and *bri1*/BRI1$_{K25R}$-mCitrine plants. (**c**) Western blot analyses on *bri1*/BRI1-mCitrine and *bri1*/BRI1$_{K25R}$-mCitrine plants using an anti-GFP antibody. The asterisk indicates aspecific signals used as loading control. (**d**) Confocal microscopy analyses of *bri1*/BRI1-mCitrine and *bri1*/BRI1$_{K25R}$-mCitrine roots. (**e**) Sensitivity of *bri1*/BRI1-mCitrine and *bri1*/BRI1$_{K25R}$-mCitrine plants to BFA. Plants were pretreated with 100μM CHX for 1 hour and exposed to 50μM BFA for 30 minutes. (**f**) Representative kymograph obtained from TIRF movies of *bri1*/BRI1-mCitrine and *bri1*/BRI1$_{K25R}$-mCitrine. The time scale is shown. (**g**) Time of residency at the plasma membrane of *bri1*/BRI1-mCitrine and *bri1*/BRI1$_{K25R}$-mCitrine. The distribution was obtained from kymograph-based track length analyses coming from 3 independent experiments (n=350). (**h**) Sensitivity of *bri1*/BRI1-

mCitrine and *bri1*/BRI1$_{K25R}$-mCitrine plants to dark growth conditions. Light-grown seedlings were kept in the dark for 2 hours before confocal imaging. See also Figure S4.